THE JOURNAL OF PHYSICAL CHEMISTRY C
A JOURNAL OF THE AMERICAN CHEMICAL SOCIETY

pubs.acs.org/JPCC

Article

Molecular Dynamics in $Ag_2B_{12}H_{12}$ Studied by Nuclear Magnetic Resonance

Published as part of The Journal of Physical Chemistry virtual special issue "Advanced Characterization by Solid-State NMR and In Situ Technology".

Anton Gradišek,* Mathias Jørgensen, Mark Paskevicius, Bjarne R. S. Hansen, and Torben R. Jensen

Cite This: *J. Phys. Chem. C* 2021, 125, 5534−5541

Read Online

ACCESS | Metrics & More | Article Recommendations

ABSTRACT: We present a molecular dynamics study of the low-temperature polymorph of silver *closo*-borate α-$Ag_2B_{12}H_{12}$, which is a promising ionic conductor. By means of ^1H and ^{11}B nuclear magnetic resonance spectroscopy, we identified two dynamic processes in the system that involve the movements of $B_{12}H_{12}^{2-}$ cages: fast rotations with an activation energy of 308 meV and tumbling of the cages at lower temperatures with an activation energy of 67 meV. Fast rotations are known to facilitate the diffusion of Ag^+ ions (the activation energy of 482 meV for ion jumps was determined from solid-state ionic conductivity measurements) while the tumbling motions are likely made possible by either impurities or local disorder, allowing for easier reorientations of the boron cages.

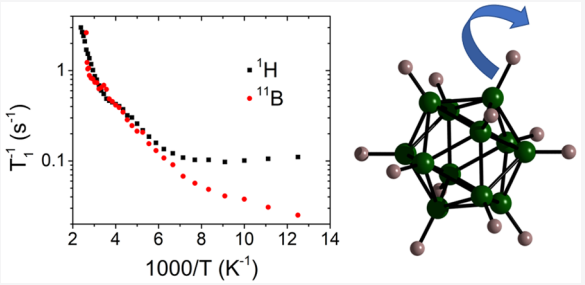

INTRODUCTION

Metal *closo*-borates form an emerging class of solid electrolytes, showing high thermal, chemical, and electrochemical stability as well as superionic conductivity in their disordered state.[1−5] Generally, the compounds exist with an ordered crystal structure at room temperature (RT) and undergo a thermally induced order−disorder transition, in which both the anion and cation sublattices become disordered as the large anion cages are distributed over two crystallographic positions. This liquid-like environment allows the cations to easily move in the structure, resulting in a sharp, order of magnitude increase in the ionic conductivity.[1,3,4] In past years, metal borates have been studied as highly promising solid state ionic conductors,[1,2,4] of special interest for fuel cells that can operate at intermediate temperatures (~300 °C) or for solid-state battery applications.[2,6,7] Some of the *closo*-borates with excellent ionic conductivity include $Li_2B_nH_n$, $Na_2B_nH_n$,[4,5] $Ag_2B_nH_n$[1] (n = 10, 12), mixed-anion compounds, such as $Ag_{(2+x)}I_xB_nH_n$[1] or $Na_3BH_4B_{12}H_{12}$,[8] and the carborates $NaCB_{11}H_{12}$ or $NaCB_9H_{10}$,[9,10] while $(NH_4)_2B_nH_n$ were found to exhibit much lower conductivities, likely because of the larger mobile ion (NH_4^+).[11,12] Recently, a system with the cation complex $N_2H_7^+$ was stabilized in the solid state.[13] Research interest has also focused on systems where hydrogen in the anion cages is replaced with a halogen (such as $B_{12}H_{12}$ or $B_{12}Cl_{12}$).[14]

Nuclear magnetic resonance (NMR) is a versatile technique that allows us to study different types of dynamic processes taking place over a wide range of time scales. Although it is a bulk method, NMR spectra can unveil the information about the local structure of the NMR-sensitive nuclei, while the spin−lattice relaxation measurements offer insight into the fluctuations of dipolar and quadrupolar interactions, which result from local and long-range motions. In boron−hydrogen compounds, NMR has often been employed to study the local rotations/reorientations of BH_4 tetrahedra.[15−19] An interesting finding in these studies is that the BH_4 tetrahedra can rotate about different crystallographic axes, and it is possible to determine the activation energies for each rotational mode from the temperature-dependent measurements of spin−lattice relaxation times, of either protons or boron. A similar approach was followed in the studies of decaborates and dodecaborates, where the rotating units are large boron cages. A study of atomic motion in $A_2B_{12}H_{12}$ (A = Na, K, Rb, Cs) unveiled that the activation energy for rotations decreases with increasing lattice parameter,[20] while the studies of $(NH_4)_2B_nH_n$ (n = 10, 12) showed that the activation energy is smaller for the $B_{10}H_{10}$ cage due to a smaller number of hydrogen atoms changing position (thus breaking the bonds) at each rotation.

Received: January 20, 2021
Revised: February 23, 2021
Published: March 4, 2021

https://dx.doi.org/10.1021/acs.jpcc.1c00528
J. Phys. Chem. C 2021, 125, 5534−5541

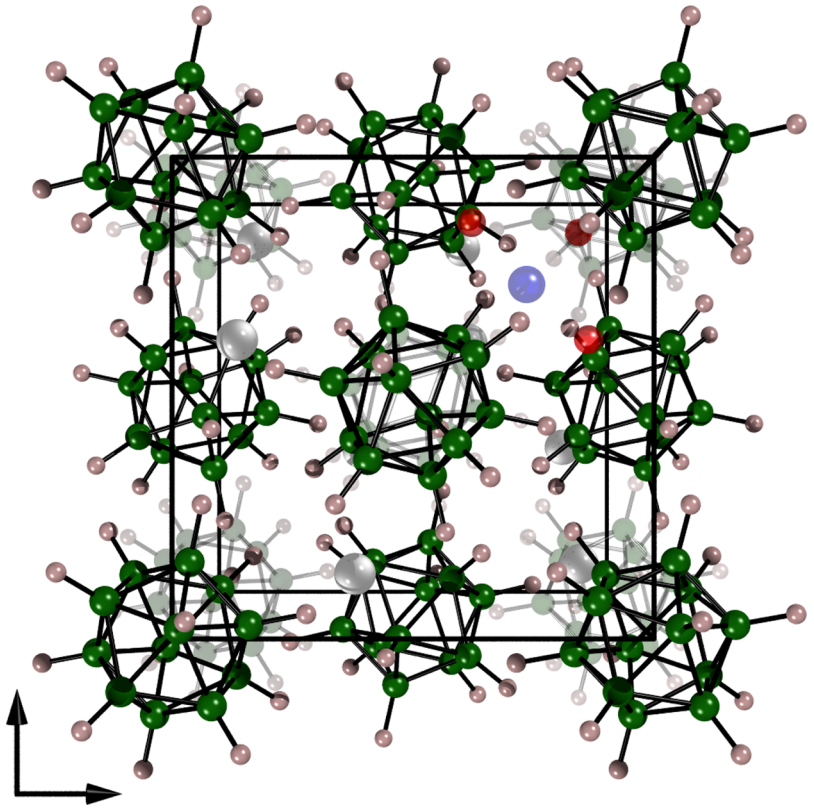

Figure 1. Crystal structure of $Ag_2B_{12}H_{12}$ in *Pa*-3, viewed down the *c*-axis. Atoms displayed include B (green), H (pink), and Ag (silver). Interstitial sites are shown in top right corner: tetrahedral in blue and trigonal in red.

In $(NH_4)_2B_nH_n$ (n = 10, 12), rotational tunneling of the NH_4 cations was observed at the lowest temperatures.[11,12,21,22] In parallel, several recent studies using *ab initio* calculations also showed strong indications that the reorientations of large boron cages can facilitate the mobility of cations.[10,23−26] Our previous studies of $Ag_2B_nH_n$ (n = 10, 12)[1] presented strong crystallographic evidence of the so-called paddle-wheel cation conductivity mechanism. The structures of the high-temperature polymorphs, β-$Ag_2B_nH_n$, reveal that only some of the available Ag positions are allowed to be occupied for a specific orientation of the *closo*-borate anion because some of the positions will result in unacceptably short Ag−H distances. Thus, as the anion changes orientation, the cations may have to move as well, or vice versa. Additionally, an NMR investigation of $LiLa(BH_4)_3Cl$ revealed that BH_4^- dynamics and Li^+ translational motion occur on the same frequency scale, further supporting a correlation between anion rotation and cation motion.[17]

Here we report an ^1H and ^{11}B NMR study by means of NMR spectra and spin−lattice relaxation measurements for both nuclei in the low-temperature polymorph of α-$Ag_2B_{12}H_{12}$. We analyze the results in view of rotations/reorientations of boron cages and diffusion of Ag^+ ions, where the latter process was previously studied by electrochemical impedance spectroscopy (EIS).

STRUCTURAL CONSIDERATIONS

The crystal structure of $Ag_2B_{12}H_{12}$, shown in Figure 1, is isostructural to $Li_2B_{12}H_{12}$, with a cubic unit cell and space group *Pa*-3, which has been studied previously.[27] The anions are situated on a face-centered sublattice while the cations are positioned in trigonal sites, slightly off-plane away from the center of the anion tetrahedra. This leaves several potential sites open to Ag, such as the corresponding off-plane trigonal site toward the center of the anion tetrahedra as well as the tetrahedral site, both of which are occupied in the disordered high-temperature polymorph.

EXPERIMENTAL DETAILS

Synthesis. $Li_2B_{12}H_{12}$ (Katchem) was dissolved in Milli-Q grade water and passed through an Amberlite IR120-H ion-exchange resin (Fluka) to form $(H_3O)_2B_{12}H_{12}$. Stoichiometric amounts of $AgNO_3$ were dissolved in Milli-Q grade water and added to the mixture under stirring. An off-white precipitate of $Ag_2B_{12}H_{12}$ immediately precipitated. Excess water was removed under dynamic vacuum at 70 °C.

Nuclear Magnetic Resonance Measurements. The sample was sealed in a quartz tube under an Ar atmosphere to prevent the contact with water vapor or oxygen and stored in dark to prevent light exposure due to photosensitivity.[1] ^1H and ^{11}B NMR spectra and spin−lattice relaxation times were measured as a function of temperature—in a heating run from 80 to 420 K (proton) and to 380 K (boron). ^1H measurements were conducted at a superconducting magnet with the field of 2.35 T (corresponding to the Larmor frequency $\nu_L(^1H)$ = 100 MHz) while the ^{11}B measurements were conducted in a setup with a field of 4.7 T, corresponding to $\nu_L(^{11}B)$ = 64.2 MHz. The temperature was controlled by using a gas-flow cryostat. NMR spectra were recorded by using $90_x-\tau-90_y$ spin echoes. Spin-relaxation times were measured by using the saturation−recovery pulse sequence. Following the measurements, the sample was checked again by using PXD to ensure that no structure changes occurred due to heating.

https://dx.doi.org/10.1021/acs.jpcc.1c00528
J. Phys. Chem. C 2021, 125, 5534−5541

RESULTS

NMR Spectra. Figure 2 shows the temperature evolution of ^{1}H and ^{11}B NMR spectra. Both spectra show similar features. At low temperatures (below 200 K), the proton spectra have a roughly Gaussian shape, with full width at half-maximum $\nu_{1/2}$ =

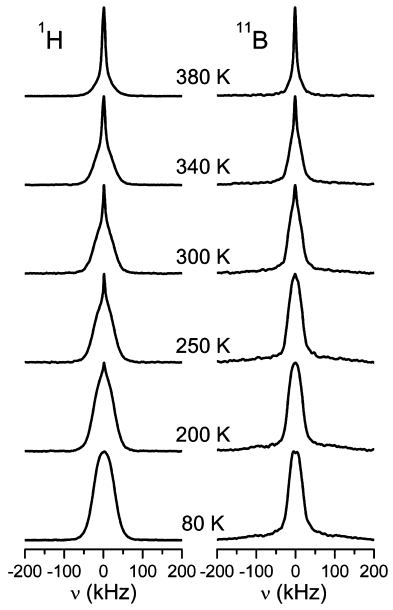

Figure 2. Temperature dependencies of the spectra for ^{1}H and ^{11}B in $Ag_2B_{12}H_{12}$, measured at 2.35 and 4.7 T, respectively.

58 kHz. Upon heating, the spectra gradually narrow. Above around 200 K, a narrow component first appears superimposed upon the broad line. With further heating, the line narrows altogether and reaches a plateau of about $\nu_{1/2}$ = 10 kHz at high temperatures. A similar effect can be seen in boron.

Spin−Lattice Relaxation. Figure 3 shows temperature dependence of ^{1}H and ^{11}B spin−lattice relaxation rates ($R_1 = 1/T_1$). Magnetization recovery in proton relaxation was found to be monoexponential throughout the temperature range while the boron relaxation was better described by using a stretch-exponent function. There was no observable difference between cooling or heating runs (at some selected temperatures). Relaxation rates for both nuclei show mostly common

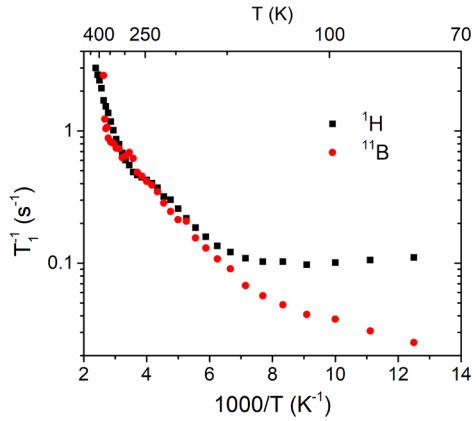

Figure 3. Temperature dependencies of spin−lattice relaxation rate for ^{1}H and ^{11}B in $Ag_2B_{12}H_{12}$.

features—in the high-temperature region (above 200 K, not to be mistaken with the high-temperature polymorph) the relaxation rate is quickly increasing with the temperature, while it levels off to a plateau at lower temperatures (more prominently seen in protons).

ANALYSIS AND DISCUSSION

We analyze the dynamics in $Ag_2B_{12}H_{12}$ in view of several similar systems, especially the isostructural $Li_2B_{12}H_{12}$. Generally, metal *closo*-borates show two distinct polymorphs: an ordered low-temperature and a disordered high-temperature polymorph. From EIS these polymorphs are clearly distinguishable, e.g., by the decrease in apparent activation energy (slope of the curve) in the HT-polymorph. Furthermore, the transition from one polymorph to the other is usually accompanied by one or several orders of magnitude change in ionic conductivity, as it is clearly seen in Figure 4, which shows the temperature dependence of ionic conductivity for $Ag_2B_{12}H_{12}$ compared to other selected compounds. In our NMR study, we only focus on the low-temperature polymorph. The activation energy for jumps of Ag^+

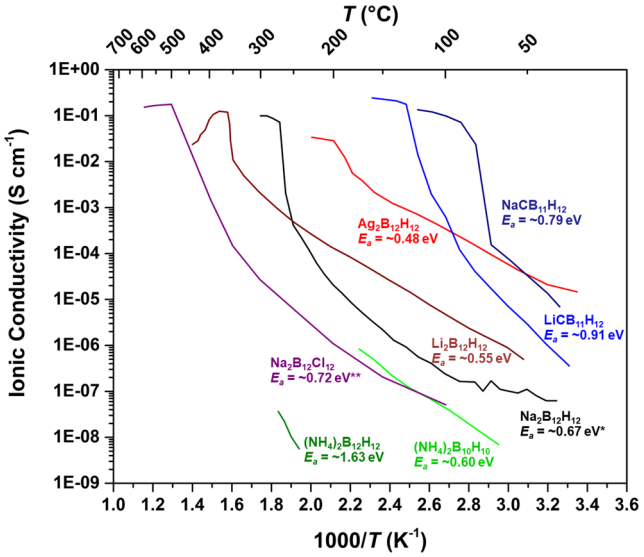

Figure 4. Ionic conductivity as a function of temperature for $Ag_2B_{12}H_{12}$ and some selected systems. The numbers, E_a, correspond to the activation energy determined from the EIS data. In case there is a jump in conductivity, the activation energy is that of the low-temperature polymorph. *,**Because of a nonlinear slope, the activation energy was determined based on a more linear subset of the data, from 150−220 and 150−300 °C, respectively.[1,6,9,11,28,29]

ions is 482 meV, which is close to the value of 550 meV for $Li_2B_{12}H_{12}$ for jumps of Li^+. On the other hand, the ionic conductivity is about 2 orders of magnitude faster in $Ag_2B_{12}H_{12}$, and the phase transition to the high-temperature polymorph occurs at a substantially lower temperature.

The shape of the proton NMR spectra is determined by the dipolar nuclear coupling, either homonuclear (proton−proton) or heteronuclear (proton−boron and proton−silver). At low temperatures, we may view the system as static, with very limited local thermal motion—resulting in broad spectra. With increasing temperature, boron cages begin to reorientate and silver ions start jumping between sites. In principle, both effects cause partial averaging of the dipolar interaction, resulting in NMR line narrowing. However, as the gyromagnetic ratio of either of the two Ag isotopes is much lower than those of proton

https://dx.doi.org/10.1021/acs.jpcc.1c00528
J. Phys. Chem. C 2021, 125, 5534−5541

or boron, we can safely assume that the main contribution to the line narrowing comes from the averaging of proton−proton and proton−boron interactions. Up to about 200 K, the line spectra are broad. Above this temperature, a narrow line superimposed on the broad line indicates that a minor part of the spectrum exhibits the narrowing, which should be related to some reorientational process. At yet higher temperatures, the line narrows further, which is the consequence of fast rotations of boron cages that average out a large part of the dipole interactions. In the case of isotropic, liquid-like motions, the spectra should exhibit a Lorentzian shape, with the line width related only to the inhomogeneity of the magnetic field. However, in our case, the spectra are not Lorentzian even at the highest temperatures, indicating only partial averaging of intermolecular interactions. This is consistent with the fact that even if they are close to spherical in shape, the $B_{12}H_{12}$ cages still have preferential reorientational axes, such as C_2, C_3, and C_5.[30]

The shape of the ^{11}B spectra, with boron being a quadrupole nucleus with a spin of 3/2, is also affected by the interactions of the electric quadrupole moment of boron nuclei with the electric field gradient (EFG) tensor generated by the surrounding atoms. As seen in Figure 2, the boron spectra at low temperatures consist of a strong central line and weak unresolved satellite transitions. Upon heating, in line with the trends seen in the proton spectra, the central transition line narrows due to the dynamic processes in the system. A minor component sees narrowing before the entire line, as in the case of the proton spectra.

Proton relaxation is governed by fluctuations of homonuclear (H−H) and heteronuclear (H−B and H−Ag) dipolar spin interactions. As in the analysis of the NMR spectra, we treat the H−Ag contribution as negligible compared to the other two. Homonuclear interaction is usually interpreted in terms of the so-called BPP model developed by Bloembergen, Purcell, and Pound.[31] The model assumes an exponential correlation function for random dipolar field fluctuations, which is characterized by a single correlation time and can be written as

$$R_1^{\mathrm{H}} = \frac{2\Delta M_{\mathrm{HH}}}{3}\left[\frac{\tau}{1+\omega_{\mathrm{H}}{}^2\tau^2} + \frac{4\tau}{1+4\omega_{\mathrm{H}}{}^2\tau^2}\right] \quad (1)$$

The heteronuclear contribution was analyzed in detail by Abragam.[32] The relaxation of spin I due to the interaction with spin S can be expressed as

$$R_1^{\mathrm{IS}} = \frac{\Delta M_{\mathrm{IS}}}{2}\left[\frac{\tau}{1+(\omega_{\mathrm{I}}-\omega_{\mathrm{S}})^2\tau^2} + \frac{3\tau}{1+\omega_{\mathrm{I}}{}^2\tau^2} + \frac{6\tau}{1+(\omega_{\mathrm{I}}+\omega_{\mathrm{S}})^2\tau^2}\right] \quad (2)$$

In the preceding expressions, ΔM_{HH} and ΔM_{IS} are the fluctuating parts of the second moments due to the homonuclear or heteronuclear interactions. $\omega_i = 2\pi\nu_i$ are the Larmor frequencies whereas τ^{-1} is the jump rate. The model assumes that τ has an Arrhenius-like temperature dependence

$$\tau = \tau_0 \exp(E_a/k_B T) \quad (3)$$

where $\tau_0{}^{-1}$ is the attempt frequency and E_a is the activation energy for rotations/reorientations. k_B is the Boltzmann constant.

On the other hand, there are two major mechanisms that influence the relaxation of ^{11}B, a quadrupole nucleus with a spin of 3/2. Similar to the proton relaxation, we take into account the fluctuations in dipolar interactions, both homonuclear and heteronuclear (although the B−B and B−Ag interactions are orders of magnitude smaller than the B−H interactions). In addition, relaxation is also influenced by fluctuations of the interaction between the nuclear quadrupole moment of boron nuclei and the electric field gradient (EFG) tensor at the site of the nuclei. In line with previous research,[11,12] we use a simple BPP-like model (eq 1) for boron relaxation, where we use M as a prefactor instead of $2\Delta M_{\mathrm{HH}}/3$.

In the above models, the spin−lattice relaxation rate exhibits a maximum in the region where $\omega\tau \sim 1$. Far from the maximum (where $\omega\tau \gg 1$ or $\omega\tau \ll 1$), the relaxation can be approximated in the asymptotic form as

$$R_1 = C \exp\left(\pm\frac{E_a}{k_B T}\right) \quad (4)$$

where $C \sim 1/\omega^2\tau_0$ for $\omega\tau \gg 1$ and $C \sim \tau_0$ for $\omega\tau \ll 1$. Drawing a comparison to borohydrides, there is often more than one dynamic mode possible in the system, and each of these modes can be described by a separate contribution to the relaxation.[15,16,18]

The R_1 curves for both nuclei at low temperatures level off toward a plateau (more clear for protons). This phenomenon can be attributed to an additional process—the relaxation due to interactions with paramagnetic impurities which are unavoidably present in the sample. This contribution is usually treated as temperature independent; thus, we add a constant $D_p^{\{H,B\}}$ to each relaxation model.

Looking at the relaxation data, it is clear that any of the two relaxation curves cannot be described by using solely a single reorientation mode together with a paramagnetic contribution; at least two dynamic contributions are required. Fitting the relaxation models to the experimental data was performed by using a nonlinear least-squares minimization with a global minimum target.[33] As the same dynamic processes affect both proton and boron relaxation, the key parameters of both models, i.e., the activation energies for rotations/reorientations of $B_{12}H_{12}$ cages as well as the associated correlation times, should be the same. As there are no obvious peaks in either relaxation curve, the simplest relaxation model assumes three contributions for relaxation of each nucleus—two associated with rotations/reorientations with the activation energies E_1 and E_2, both in the slow-motion limit, as well as a constant term due to paramagnetic impurities. This model yields the values of E_1 = 314 meV and E_2 = 60 meV, and the model curves (not shown) match the experimental points reasonably well.

On the basis of this simple model, it is clear that one of the dynamic modes (with E_1) becomes visible only at the highest temperatures, and it is thus only reasonable to describe it in the limit approximation (eq 4). On the other hand, we can use a BPP-like model (eq 1) to describe the dynamic mode that is more prominent at lower temperature (with E_2) to further improve the model. An additional parameter in this model is the correlation time, τ_0, and the feature of this model is that it exhibits a local maximum. The results of this model fit are shown in Figures 5 and 6. Here, we obtain the following parameters: for the high-temperature mode in the limit approximation, we get E_1 = 308 meV and the prefactors $C^{\mathrm{H}} = 1.2 \times 10^4\ \mathrm{s}^{-1}$ for protons and $C_{\mathrm{B}} = 7.4 \times 10^3\ \mathrm{s}^{-1}$ for boron. For the second dynamic mode, with a BPP-like model, we get E_2 = 67 meV, $\tau_0 = 2.2 \times 10^{-10}$ s, and the prefactors $M_{\mathrm{H}} = 3.1 \times 10^8\ \mathrm{s}^{-2}$ for protons and $M_{\mathrm{B}} = 1.8 \times 10^8\ \mathrm{s}^{-2}$

https://dx.doi.org/10.1021/acs.jpcc.1c00528
J. Phys. Chem. C 2021, 125, 5534−5541

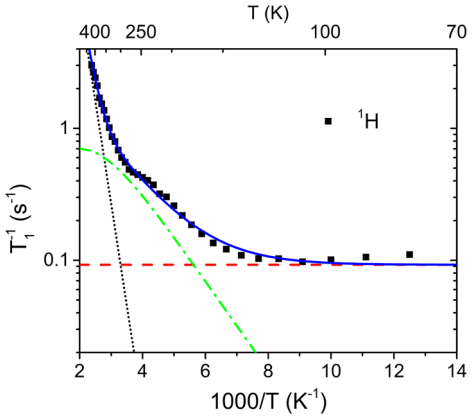

Figure 5. ^{1}H spin−lattice relaxation rates as a function of inverse temperature. Lines represent individual contributions to relaxation, obtained by the best fit to the experimental data: fast rotations of boron cages with E_1 (dots), slower dynamic mode with E_2 (dash-dot line), paramagnetic impurities (dashed line), and total relaxation (solid line).

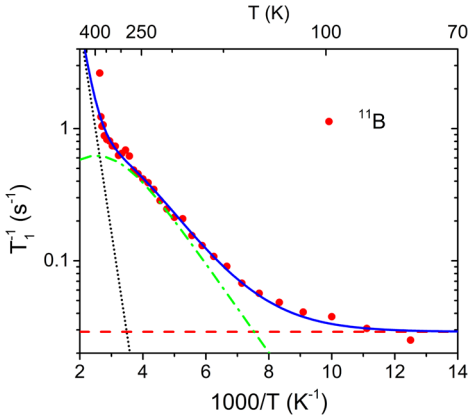

Figure 6. ^{11}B spin−lattice relaxation rates as a function of inverse temperature. Lines represent individual contributions to relaxation, obtained by the best fit to the experimental data: fast rotations of boron cages with E_1 (dots), slower dynamic mode with E_2 (dash-dot line), paramagnetic impurities (dashed line), and total relaxation (solid line).

for boron. The constant contributions of the paramagnetic impurities are $D_p^H = 0.092$ s^{-1} and $D_p^B = 0.029$ s^{-1}. In view of root-mean-square error (RMSE), there is little difference between both models, by using either only the slow-motion limit approximations or a BPP-like model for the low-temperature mode. This shows that the first model already describes the relevant features sufficiently well and that the use of a BPP-like model can only give us an approximate value of τ_0.

At this point, we can compare the activation energies in $Ag_2B_{12}H_{12}$ with those of similar of *closo*-borates and related systems. The value of $E_1 = 308$ meV is within the range of values for fast rotations/reorientations of boron cages in several similar systems. For comparison, the activation energies for this process, obtained by means of NMR spectroscopy, were 480 and 236 meV in $(NH_4)_2B_{12}H_{12}$ and $(NH_4)_2B_{10}H_{10}$, respectively,[11] 409 meV for $LiCB_{11}H_{12}$,[34] 302 meV for $LiCB_9H_{10}$,[35] and so on. The activation energy in $Li_2B_{12}H_{12}$ is a staggering 1400 meV,[5] but the value for this compound appears to be an outlier among similar systems. It is thus reasonable to assign the process in $Ag_2B_{12}H_{12}$ with E_1 to fast rotations/reorientations of boron cages as well. Skripov et al.[20] found that the activation energy in $A_2B_{12}H_{12}$-type systems decreases with increasing cation radius; similar effects were observed by Tiritiris et al.[36] A common feature in *closo*-borates and related systems is that the activation energies for rotations of boron cages substantially drop upon the transition from the ordered low-temperature polymorph to the high-temperature one with a higher level of disorder. For example, in $Na_2B_{12}H_{12}$, it drops from 770 to 270 meV upon the transition.[20]

Returning to the connection between the activation energies for rotations of boron cages and those for cation jumps obtained by ionic conductivity measurements (EIS), a common feature appears to be that a higher activation energy is required for jumps than for the cage reorientation. In $Ag_2B_{12}H_{12}$, we have 482 meV for Ag^+ jumps and 308 meV for reorientations. In $(NH_4)_2B_{10}H_{10}$, the values are 600 meV vs 236 meV and in $(NH_4)_2B_{12}H_{12}$ 1.63 eV vs 480 meV.[11] Then, we have 720 meV vs 450 meV in the LT phase of $Na_2B_{12}H_{12}$, 790 meV vs 409 meV in the LT phase of $NaCB_{11}H_{12}$,[34] and 910 meV vs 409 meV in the LT phase of $LiCB_{11}H_{12}$.[34] The difference is likely attributed to the fact that the detaching of the cation (defect creation) and a subsequent jump require more energy than just the rotation of the boron cage that otherwise leaves the surroundings unchanged. Again, $Li_2B_{12}H_{12}$ is an outlier here, with the activation energy for rotations (1400 meV) being *larger* than the value for diffusion (550 meV). Skripov et al. provide a good overview of activation energies for both diffusion and reorientations in ref 19; however, the activation energies for diffusion listed there were determined by using methods of NMR spectroscopy and may thus differ from the EIS measurements.

The relatively low activation energy of anion rotation in $Ag_2B_{12}H_{12}$ compared with similar compounds may be explained by the more polarizing nature of Ag, resulting in a more covalent bond character. Owing to this, the interstitial cation sites (Frenkel defects) are less destabilized by surrounding cations compared to, for example, Li^+ and Na^+ which tend to form bonds of more ionic character. This is similar to how AgCl tends to form Frenkel defects,[37] whereas NaCl predominantly forms Schottky defects.[38] As such, the interstitial sites (e.g., tetrahedral sites) are likely occupied to a larger extent in the low-temperature polymorph of $Ag_2B_{12}H_{12}$ compared with those of the alkali metal *closo*-borates. This may enable easier reorientation of the boron cage similar to the HT-polymorph, albeit less frequent. On the other hand, the activation energies for anion reorientation between alkali metal and Ag *closo*-borates could be related to innate bonding differences in cation−anion interactions.

While the process with E_1 fits well into the picture as fast rotations/reorientations of $B_{12}H_{12}$ cages, the nature of the process with E_2 = 67 meV is somewhat less obvious. The activation energy is much lower than the values for any type of fast anion rotations, which are typically well above 100 meV.[19] In certain borohydrides and *closo*-borates, low-temperature motions were observed with activation energies in the order of tens of meV.[11,12,17,18] These processes were attributed to rotational tunneling of BH_4, NH_4, or NH_3 units. While E_2 seems closer to the activation energies for these processes, the temperature range where they occur is different. Relaxation in systems that exhibit rotational tunneling always exhibits a peak well below 100 K while the peak of the process with E_2 is above 300 K (see Figures 5 and 6). Thus, this process takes place well into the thermally activated region as opposed to quantum phenomena occurring at low temperatures. The process with E_2 should be nevertheless connected to some sort of movements of

https://dx.doi.org/10.1021/acs.jpcc.1c00528
J. Phys. Chem. C 2021, 125, 5534−5541

$B_{12}H_{12}$ cages, such as tumbling or twitching of the cages instead of full thermally activated rotations. It appears that only a small fraction of the cages undergoes such motions. Looking at the NMR spectra, such motions would explain the narrow peak that appears before the main broad proton line starts narrowing upon heating—tumbling motions do partially average out the dipolar interactions. This assumption can be also backed by looking at the relaxation data. The peak attributed to the process with E_2 has a much lower amplitude than that of the process with E_1 (where the peak is not even reached). E_2 being considerably smaller than E_1 suggests that the tumbling cages are more loosely bound to the structure than the rest. From the PXD data, we only see the single-phase α-$Ag_2B_{12}H_{12}$ in this temperature range (see the Supporting Information in ref 1 for PXD at room temperature), which rules out a biphasic system. However, it is possible that some disorder (perhaps similar to that in the high-temperature polymorph) exists at grain boundaries, which would not be visible by PXD. It has recently been identified that interfacial/grain boundaries in Li−B−H based solid-state electrolytes could provide regions of exceptional ionic conductivity in ball-milled or composite materials.[39,40] As such, mechanical modification of solid-state ionic conductors can lead to two regions displaying different degrees of ionic conductivity, which may be due to the formation and stabilization of a different crystallographic polymorph or a nano/noncrystalline structure type. Although no ball-milling or deliberate structural modification were undertaken in the present research, it is possible that the rapidly precipitated $Ag_2B_{12}H_{12}$ displays nanoscale structural variations, possibly due to small particle size,[1] that could explain the two types of reorientational motion observed. An additional possibility is that the tumbling of cages is facilitated by impurities in the system, again on the nanoscale and thus not seen by PXD. $Ag_2B_{12}H_{12}$ is sensitive to light and forms Ag metal nanoparticles/wires during synthesis and subsequent handling,[1] though it is not yet entirely clear what happens to the $B_{12}H_{12}^{2-}$ part when this occurs. Such a reaction does not take place in $Li_2B_{12}H_{12}$. As NMR studies of dynamics in *closo*-borates and related systems typically focus on the analysis of the temperature range where fast rotations of boron cages are the dominant mechanism (and do not report/study the behavior at lower temperatures), it is difficult to conclude whether the process with E_2 we see in $Ag_2B_{12}H_{12}$ is a typical feature related to the disorder at the grain boundaries or whether it is a peculiarity of this system due to its photosensitivity. Further research is required to fully answer this question.

SUMMARY AND CONCLUSIONS

We studied molecular dynamics in the low-temperature polymorph of $AgB_{12}H_{12}$, a *closo*-borate system with promising ionic conductivity, by means of ^1H and ^{11}B NMR spectra and spin−lattice relaxation. Fast rotations/reorientations of $B_{12}H_{12}$ cages were identified to have an activation energy of 308 meV, which ranks among the lower values for low-temperature polymorphs of several *closo*-borates and related systems. This could be attributed to the polarizing nature of Ag, which may cause a more disordered occupancy of available interstitial sites, thus allowing for easier reorientations of the boron cages. Rotations of boron cages assist the jumping of Ag^+ ions, although the activation energy for this process (determined by solid-state ionic conductivity measurements) is larger, at 482 meV. The reason is that the jump of a silver ion creates a defect in the lattice which requires additional energy. An additional dynamic process was identified, with a relatively low activation energy of 67 meV. This process is likely linked to the tumbling motion of $B_{12}H_{12}$ cages, either in locally disordered environments or due to the impurities that have formed in the photosensitive sample during synthesis and handling. Both dynamic processes cause partial averaging of the dipolar nuclear interactions, which is seen as the narrowing of proton and boron NMR spectra upon increasing the temperature.

Because of the limitations in the experimental equipment, only the dynamics in the low-temperature polymorph was studied. A detailed analysis of the high-temperature polymorph, with a significantly higher ionic conductivity, remains for future studies.

AUTHOR INFORMATION

Corresponding Author

Anton Gradišek − *Jožef Stefan Institute, SI-1000 Ljubljana, Slovenia;* orcid.org/0000-0001-6480-9587; Phone: +386 1 477 3967; Email: anton.gradisek@ijs.si

Authors

Mathias Jørgensen − *Interdisciplinary Nanoscience Center (iNANO), Department of Chemistry, Aarhus University, DK-8000 Aarhus, Denmark*

Mark Paskevicius − *Interdisciplinary Nanoscience Center (iNANO), Department of Chemistry, Aarhus University, DK-8000 Aarhus, Denmark; Department of Physics and Astronomy, Fuels and Energy Technology Institute, Curtin University, Perth, WA 6845, Australia;* orcid.org/0000-0003-2677-3434

Bjarne R. S. Hansen − *Interdisciplinary Nanoscience Center (iNANO), Department of Chemistry, Aarhus University, DK-8000 Aarhus, Denmark*

Torben R. Jensen − *Interdisciplinary Nanoscience Center (iNANO), Department of Chemistry, Aarhus University, DK-8000 Aarhus, Denmark;* orcid.org/0000-0002-4278-3221

Complete contact information is available at: https://pubs.acs.org/10.1021/acs.jpcc.1c00528

Notes

The authors declare no competing financial interest.

ACKNOWLEDGMENTS

A.G. acknowledges the funding of Slovenian Research Agency, Grants P1-0125 and P2-0209. M.P. thanks the Australian Research Council for ARC Future Fellowship FT160100303. The work was supported by the Danish National Research Foundation, Center for Materials Crystallography (DNRF93), the Danish Council for Independent Research, Nature and Universe (Danscatt), and Technology and Production (HyNanoBorN, DFF4181-00462), and the Carlsberg Foundation. Affiliation with the Center for Integrated Materials Research (iMAT) at Aarhus University is gratefully acknowledged. We also thank the anonymous reviewers for their comments.

REFERENCES

(1) Paskevicius, M.; Hansen, B. R.; Jørgensen, M.; Richter, B.; Jensen, T. R. Multifunctionality of silver closo-boranes. *Nat. Commun.* **2017**, *8*, 1−6.

(2) Hansen, B. R.; Paskevicius, M.; Li, H.-W.; Akiba, E.; Jensen, T. R. Metal boranes: Progress and applications. *Coord. Chem. Rev.* **2016**, *323*, 60−70.

(3) Udovic, T. J.; Matsuo, M.; Tang, W. S.; Wu, H.; Stavila, V.; Soloninin, A. V.; Skoryunov, R. V.; Babanova, O. A.; Skripov, A. V.; Rush, J. J.; et al. Exceptional Superionic Conductivity in Disordered Sodium Decahydro-closo-decaborate. *Adv. Mater.* **2014**, *26*, 7622−7626.
(4) He, L.; Li, H.-W.; Nakajima, H.; Tumanov, N.; Filinchuk, Y.; Hwang, S.-J.; Sharma, M.; Hagemann, H.; Akiba, E. Synthesis of a bimetallic dodecaborate LiNaB12H12 with outstanding superionic conductivity. *Chem. Mater.* **2015**, *27*, 5483−5486.
(5) Verdal, N.; Her, J.-H.; Stavila, V.; Soloninin, A. V.; Babanova, O. A.; Skripov, A. V.; Udovic, T. J.; Rush, J. J. Complex high-temperature phase transitions in Li2B12H12 and Na2B12H12. *J. Solid State Chem.* **2014**, *212*, 81−91.
(6) Paskevicius, M.; Jepsen, L. H.; Schouwink, P.; Černỳ, R.; Ravnsbæk, D. B.; Filinchuk, Y.; Dornheim, M.; Besenbacher, F.; Jensen, T. R. Metal borohydrides and derivatives-synthesis, structure and properties. *Chem. Soc. Rev.* **2017**, *46*, 1565−1634.
(7) Tang, W. S.; Unemoto, A.; Zhou, W.; Stavila, V.; Matsuo, M.; Wu, H.; Orimo, S.-i.; Udovic, T. J. Unparalleled lithium and sodium superionic conduction in solid electrolytes with large monovalent cage-like anions. *Energy Environ. Sci.* **2015**, *8*, 3637−3645.
(8) Sadikin, Y.; Brighi, M.; Schouwink, P.; Černỳ, R. Superionic Conduction of Sodium and Lithium in Anion-Mixed Hydroborates Na3BH4B12H12 and (Li0. 7Na0. 3) 3BH4B12H12. *Adv. Energy Mater.* **2015**, *5*, 1501016.
(9) Tang, W. S.; Matsuo, M.; Wu, H.; Stavila, V.; Zhou, W.; Talin, A. A.; Soloninin, A. V.; Skoryunov, R. V.; Babanova, O. A.; Skripov, A. V.; et al. Liquid-like ionic conduction in solid lithium and sodium monocarba-closo-decaborates near or at room temperature. *Adv. Energy Mater.* **2016**, *6*, 1502237.
(10) Jørgensen, M.; Shea, P. T.; Tomich, A. W.; Varley, J. B.; Bercx, M.; Lovera, S.; Cerny, R.; Zhou, W.; Udovic, T. J.; Lavallo, V.; et al. Understanding Superionic Conductivity in Lithium and Sodium Salts of Weakly Coordinating Closo-Hexahalocarbaborate Anions. *Chem. Mater.* **2020**, *32*, 1475−1487.
(11) Gradišek, A.; Krnel, M.; Paskevicius, M.; Hansen, B. R.; Jensen, T. R.; Dolinšek, J. Reorientational Motions and Ionic Conductivity in (NH4) 2B10H10 and (NH4) 2B12H12. *J. Phys. Chem. C* **2018**, *122*, 17073−17079.
(12) Skripov, A. V.; Skoryunov, R. V.; Soloninin, A. V.; Babanova, O. A.; Stavila, V.; Udovic, T. J. Nuclear Magnetic Resonance Study of Anion and Cation Reorientational Dynamics in (NH4)2B12H12. *J. Phys. Chem. C* **2018**, *122*, 3256−3262.
(13) Grinderslev, J. B.; Lee, Y.-S.; Paskevicius, M.; Møller, K. T.; Yan, Y.; Cho, Y. W.; Jensen, T. R. Ammonium-Ammonia Complexes, N2H7+, in Ammonium closo-Borate Ammines: Synthesis, Structure, and Properties. *Inorg. Chem.* **2020**, *59*, 11449.
(14) Bukovsky, E. V.; Peryshkov, D. V.; Wu, H.; Zhou, W.; Tang, W. S.; Jones, W. M.; Stavila, V.; Udovic, T. J.; Strauss, S. H. Comparison of the Coordination of B12F122-, B12Cl122-, and B12H122-to Na+ in the Solid State: Crystal Structures and Thermal Behavior of Na2 (B12F12), Na2 (H_2O) 4 (B12F12), Na2 (B12Cl12), and Na2 (H_2O) 6 (B12Cl12). *Inorg. Chem.* **2017**, *56*, 4369−4379.
(15) Skripov, A. V.; Soloninin, A. V.; Babanova, O. A.; Hagemann, H.; Filinchuk, Y. Nuclear magnetic resonance study of reorientational motion in α-Mg (BH4) 2. *J. Phys. Chem. C* **2010**, *114*, 12370−12374.
(16) Gradišek, A.; Ravnsbæk, D. B.; Vrtnik, S.; Kocjan, A.; Lužnik, J.; Apih, T.; Jensen, T. R.; Skripov, A. V.; Dolinšek, J. NMR study of molecular dynamics in complex metal borohydride LiZn2 (BH4) 5. *J. Phys. Chem. C* **2013**, *117*, 21139−21147.
(17) Skripov, A. V.; Soloninin, A. V.; Ley, M. B.; Jensen, T. R.; Filinchuk, Y. Nuclear magnetic resonance studies of BH4 reorientations and Li diffusion in LiLa (BH4) 3Cl. *J. Phys. Chem. C* **2013**, *117*, 14965−14972.
(18) Gradišek, A.; Jepsen, L. H.; Jensen, T. R.; Conradi, M. S. Nuclear magnetic resonance study of molecular dynamics in ammine metal borohydride Sr (BH4) 2 (NH3) 2. *J. Phys. Chem. C* **2016**, *120*, 24646−24654.
(19) Skripov, A. V.; Soloninin, A. V.; Babanova, O. A.; Skoryunov, R. V. Anion and Cation Dynamics in Polyhydroborate Salts: NMR Studies. *Molecules* **2020**, *25*, 2940.
(20) Skripov, A. V.; Babanova, O. A.; Soloninin, A. V.; Stavila, V.; Verdal, N.; Udovic, T. J.; Rush, J. J. Nuclear magnetic resonance study of atomic motion in A2B12H12 (A= Na, K, Rb, Cs): Anion reorientations and Na+ mobility. *J. Phys. Chem. C* **2013**, *117*, 25961−25968.
(21) Andersson, M. S.; Grinderslev, J. B.; Jensen, T. R.; Sakai, V. G.; Häussermann, U.; Udovic, T. J.; Karlsson, M. Interplay of NH 4+ and BH 4- reorientational dynamics in NH4BH4. *Phys. Rev. Mater.* **2020**, *4*, 085002.
(22) Verdal, N.; Udovic, T. J.; Rush, J. J.; Stavila, V.; Wu, H.; Zhou, W.; Jenkins, T. Low-temperature tunneling and rotational dynamics of the ammonium cations in (NH4) 2B12H12. *J. Chem. Phys.* **2011**, *135*, 094501.
(23) Lu, Z.; Ciucci, F. Structural origin of the superionic Na conduction in Na2B10H10 closo-borates and enhanced conductivity by Na deficiency for high performance solid electrolytes. *J. Mater. Chem. A* **2016**, *4*, 17740−17748.
(24) Varley, J. B.; Kweon, K.; Mehta, P.; Shea, P.; Heo, T. W.; Udovic, T. J.; Stavila, V.; Wood, B. C. Understanding ionic conductivity trends in polyborane solid electrolytes from ab initio molecular dynamics. *ACS Energy Letters* **2017**, *2*, 250−255.
(25) Kweon, K. E.; Varley, J. B.; Shea, P.; Adelstein, N.; Mehta, P.; Heo, T. W.; Udovic, T. J.; Stavila, V.; Wood, B. C. Structural, chemical, and dynamical frustration: origins of superionic conductivity in closo-borate solid electrolytes. *Chem. Mater.* **2017**, *29*, 9142−9153.
(26) Dimitrievska, M.; Shea, P.; Kweon, K. E.; Bercx, M.; Varley, J. B.; Tang, W. S.; Skripov, A. V.; Stavila, V.; Udovic, T. J.; Wood, B. C. Carbon incorporation and anion dynamics as synergistic drivers for ultrafast diffusion in superionic LiCB11H12 and NaCB11H12. *Adv. Energy Mater.* **2018**, *8*, 1703422.
(27) Her, J.-H.; Yousufuddin, M.; Zhou, W.; Jalisatgi, S. S.; Kulleck, J. G.; Zan, J. A.; Hwang, S.-J.; Bowman, R. C., Jr.; Udovic, T. J. Crystal structure of Li2B12H12: a possible intermediate species in the decomposition of LiBH4. *Inorg. Chem.* **2008**, *47*, 9757−9759.
(28) Udovic, T. J.; Matsuo, M.; Unemoto, A.; Verdal, N.; Stavila, V.; Skripov, A. V.; Rush, J. J.; Takamura, H.; Orimo, S.-i. Sodium superionic conduction in Na 2 B 12 H 12. *Chem. Commun.* **2014**, *50*, 3750−3752.
(29) Hansen, B. R.; Paskevicius, M.; Jørgensen, M.; Jensen, T. R. Halogenated sodium-closo-dodecaboranes as solid-state ion conductors. *Chem. Mater.* **2017**, *29*, 3423−3430.
(30) Verdal, N.; Udovic, T. J.; Rush, J. J.; Cappelletti, R. L.; Zhou, W. Reorientational Dynamics of the Dodecahydro-closo-dodecaborate Anion in Cs2B12H12. *J. Phys. Chem. A* **2011**, *115*, 2933−2938.
(31) Bloembergen, N.; Purcell, E. M.; Pound, R. V. Relaxation effects in nuclear magnetic resonance absorption. *Phys. Rev.* **1948**, *73*, 679.
(32) Abragam, A. *The Principles of Nuclear Magnetism*; Oxford University Press: 1961.
(33) Sebastião, P. J. The art of model fitting to experimental results. *Eur. J. Phys.* **2014**, *35*, 015017.
(34) Skripov, A. V.; Skoryunov, R. V.; Soloninin, A. V.; Babanova, O. A.; Tang, W. S.; Stavila, V.; Udovic, T. J. Anion reorientations and cation diffusion in LiCB11H12 and NaCB11H12:1H, 7Li, and 23Na NMR studies. *J. Phys. Chem. C* **2015**, *119*, 26912−26918.
(35) Soloninin, A. V.; Dimitrievska, M.; Skoryunov, R. V.; Babanova, O. A.; Skripov, A. V.; Tang, W. S.; Stavila, V.; Orimo, S.-i.; Udovic, T. J. Comparison of anion reorientational dynamics in MCB9H10 and M2B10H10 (M = Li, Na) via nuclear magnetic resonance and quasielastic neutron scattering studies. *J. Phys. Chem. C* **2017**, *121*, 1000−1012.
(36) Tiritiris, I.; Schleid, T.; Muller, K. Solid-state NMR studies on ionic closo-dodecaborates. *Appl. Magn. Reson.* **2007**, *32*, 459−481.
(37) Friauf, R. Determination of ionic transport processes in AgCl and AgBr. *J. Phys. (Paris)* **1977**, *38*, 1077−1088.
(38) Hooton, I. E.; Jacobs, P. Ionic conductivity of pure and doped sodium chloride crystals. *Can. J. Chem.* **1988**, *66*, 830−835.

https://dx.doi.org/10.1021/acs.jpcc.1c00528
J. Phys. Chem. C 2021, 125, 5534−5541

(39) Gulino, V.; Barberis, L.; Ngene, P.; Baricco, M.; de Jongh, P. E. Enhancing Li-Ion Conductivity in LiBH4-Based Solid Electrolytes by Adding Various Nanosized Oxides. *ACS Applied Energy Materials* **2020**, *3*, 4941−4948.
(40) Tang, W. S.; Matsuo, M.; Wu, H.; Stavila, V.; Unemoto, A.; Orimo, S.-i.; Udovic, T. J. Stabilizing lithium and sodium fast-ion conduction in solid polyhedral-borate salts at device-relevant temperatures. *Energy Storage Materials* **2016**, *4*, 79−83.

https://dx.doi.org/10.1021/acs.jpcc.1c00528
J. Phys. Chem. C 2021, 125, 5534−5541